Non-mesocyclone Tornadoes

Zoltán Polyánszky
Hungarian Meteorological Service
P.O. Box 38, H-1024 Budapest, Hungary
Polyanszky.z@met.hu

Gyula Bondor
Hungarian Association of Stormchasers and Storm Damage Surveyors
H-1165 Budapest, Hungary
bondor.gy@szupercella.hu

Presented at the XXX OSTIV Congress, Szeged, Hungary, 28 July - 4 August 2010

Abstract

Knowledge of environments favorable to the formation of tornadoes, even weak ones, is important to the soaring weather forecaster. Accordingly, most violent tornadoes develop usually from supercell thunderstorms. But, in Hungary, there have been damaging tornadoes which developed in environments not favorable for supercell formation (low vertical wind shear, small storm-relative Helicity). A total of 31 visual vortices from 2005 to 2009 were studied using data obtained from reports of storm spotters and the ESWD database. Eight of these vortices were classified as tornadoes (five F0, two F1, one F2), the others were funnels. To investigate these cases, several analysis fields (MSL, moisture convergence, 0-2 km vertical temperature gradient, 0-3 km section of surface based CAPE, LCL) and vertical profiles were generated from the hydrostatic run of WRF ARW 3.1.1 with horizontal resolution of 10 km and the assimilation of surface information (provided by an automatic measurement network including approximately 100 instruments operating in Hungarian Meteorological Service). The studied parameters in the environment of the cases appeared to be not significant. So, it may be assumed that these types of tornadoes are the majority of relatively weak tornadoes in Hungary. All tornadoes developed directly on stationary wind shift boundaries that generated strong convergence and pre-existing vertical vorticity circulations. These boundaries could be occluded fronts developed ahead or behind the surface cold front, along a weak quasi-stationary front or in a flat pressure area (no pressure gradient). The parent clouds of these tornadoes were usually developing cumulonimbus. The intense precipitation started usually a short time after the observation of the intense vortices. So, it may be assumed that the smaller scale thunderstorm outflow boundaries can enhance the pre-existing vertical circulations along wind shift boundaries.

Introduction

Most violent tornadoes develop usually from supercell thunderstorms. But, in Hungary, there have been damaging tornadoes that developed in environments not favorable for supercells.[1, 2, 3, 4] These types of tornadoes are generally much weaker than their mesocyclone-related cousins, but they are capable of producing damage. Wakimoto and Wilson[2] have suggested that even F3 damage is possible from these non-mesocyclone tornados. Their life cycle is different from tornadoes associated with supercells. They are preceded by a low level circulation likely originating from shearing instability and subsequently develop into a much deeper and more intense circulation under the influence of a vigorous updraft. In contrast, the supercell tornadoes are preceded by a midlevel mesocyclone well identifiable by Doppler radar and subsequent tornado development occurs when the mesocyclone intensifies at lower levels.[2] Bluestein[5] introduced the term „landspout" after he observed a weak tornado in Oklahoma which visually resembled a waterspout and developed in a non-supercell environment from a line of rapidly growing cumuli. Also, Brady and Szoke[3] presented an example of Colorado „landspout" that was visually similar to a waterspout. They associated this type of tornado mainly to non-mesocyclone processes.

The mesoscale proposed by Fujita[1] covers vorticies from 40 to 4000m in diameter. According to this scale, most tornadoes (with the exceptions of small ones) are fast-rotating mesocyclones. Mesocyclones are thought to influence the initiation of deep moist convection.[6] Lee et al.[7] show that mesocyclones along a simulated thunderstorm gustfront produces moist convective updrafts which are deeper and more intense than those for an analogous gust front without mesocyclones. During the International H2O project, the properties of the mesocyclones were analyzed to understand the role they play in the initiation of deep moist convection and non-supercell tornadoes. Mobile radars collected high-resolution data, finescale numerical model data and other observations were used for analysis. The mesocyclones

developed along mesoscale boundaries, where the maximum vertical vorticity was collocated with a radar reflectivity maximum and its field decreased with height. Enhanced low-level convergence was found at the intersections of the boundaries and mesocyclones were observed to intensify in their vicinity.[6]

Sinclar[8] noted that formative mechanism differ, some of the conditions which favour dust devil development appear to favour the formation of mesocyclone tornadoes. Dust devils arise due to the development of unstable low level lapse-rates in association with intensive diurnal surface heating. Renno[9] showed a simple thermodynamic theory for dust devils and applied it to waterspouts. The theory is based on the thermodynamics of heat engines and showed that convective vortices are more likely to form in the regions where the occurrence of the warmest and moistest updrafts and the coldest and driest downdrafts are supported by the local environment. These are the regions where both the heat input into the convective heat engine is a maximum and the solenoidal generation of vorticity is the greatest. This explains why waterspouts are frequently observed near the boundaries between relatively warm and relatively cold waters.

Keul, et al.[10] applied their North American waterspout forecasting methodology on a sample of 110 waterspout events for the years 2002–2006 over the Central-Eastern Mediterranean. They examined an instability parameter below 1500m (water – 850mb temperature difference) (- ΔT), convective cloud depth (EL – LCL difference) (- ΔZ) and 850mb wind speed. The examinations showed that the majority of waterspout cases were associated with large values of ΔZ (>8500m) and relatively small values of ΔT (<16°C). This can indicate that dynamic processes are the dominant mechanisms for waterspout development compared to thermal processes which result from thermal contrasts between the water and air. Over half of the waterspout events occurred during relatively light wind conditions (850 mb wind speed <7.5 m/s) and all waterspouts developed when the wind speed at 850 mb was less than 20 m/s. The synoptic type categorization showed a long wave ridge to the East - North East as the most frequent type associated with waterspout activity.

Non-mesocyclone tornado features and environments

Most of these tornadoes have short lifetime (5-10 min), but a few may be long-lived.[3] Twenty-seven visual vortices were examined by Wakimoto and Wilson[1] and their circulations were surface based and usually did not extend to cloud base. The parent clouds of these tornadoes were often cumuli or cumulus congestus that evolved into thunderstorms at a later stage. The precipitation echo was associated with the visual vortex in most cases and the echo intensity sometimes increased further.

This type of tornado is difficult to detect by radar. Seventeen visual vortices were detected and there was a suggestion that these vortices were usually not detectable beyond ~ 40 km [2]. The radar vortices accompanying these visual vortices were typically $\leq$ 2 km in diameter between the range of 130 and 1000m when the shear was a maximum.

The maximum depth of the circulations ranged between 0.8 and 7.9 km. The circulations are significantly smaller and shallower than the mesocyclone signatures described by Lemon et al.[11]. The signatures are often difficult to distinguish from background noise due to their small size and relatively weak Doppler velocities.[3] The reflectivity hook echo and Doppler velocity rotation signature are similar in their appearance to those often associated with supercell tornadoes, but the scale is much smaller in this case.[2]

On the basis of proximity soundings, Brady and Szoke[3] showed that the 0-6 km wind speeds and shears suggest that the tilting of ambient horizontal vorticity into vertical was not important in the formation of this circulation, moreover, it was unnecessary because vertical vorticity was already present along a mesoscale shear/convergence zone.

The observational studies by Rasmussan and Blanchard[12] indicated that a vector shear magnitude of roughly 15-20 m/s over the lowest 6 km is necessary to support a mesocyclone. Based on large RUC-2 proximity sounding samples, the 0-6 km vector shear magnitude clearly discriminated all supercells and non-supercells with no overlap in values between the 10th percentile for supercells (15 to 18 m/s) and the 90th percentile for non-supercells (~14 m/s), and differences in the means between the supercell groups and non-supercells were statistically significant.[13] Therefore, it appears likely that the areas of regular formation or interaction of low-level, mesoscale convergent/shear boundaries conducive to „active" convective development may result in preferred areas of non-mesocyclone tornado production.[3]

Caruso and Davies[4] examined six tornadoes associated with non-mesocyclone environments. In all cases, a weak, slow-moving or stationary surface front with little temperature contrast, but a sharp wind shift, was evident. The frontal wind shift boundary was important in providing low-level convergence and pre-existing low-level vertical vorticity. Along this wind shift boundary, steep 0-2 km lapse-rate (usually 9.0 – 10.0 C/km) was found to overlap substantial 0-3 km mlCAPE (mixed-layer CAPE usually 40-90 J/kg) and total CAPE, likely enhancing low-level stretching of parcels entering the storm updrafts on the boundary. In these examined cases, there was small (< 50 m^2/s^2) 0-1 km storm-relative helicity and mlCIN (mixed-layer CIN) and high mlLCL (mixed-layer LCL) (> 1600 m AGL).[14] They showed one case, when the boundary intersection area (a source of pre-existing vorticity) appeared to stay within the flanking line structure of the supercell where a F1 tornado developed. The storm-relative velocity data showed adequately the midlevel mesocyclone, but it was located several kilometers away from the reported tornado. This was a great example of a non-mesocyclone tornado that may have occured in conjunction with a supercell.

In the 70's, some studies were initiated about tornadoes and waterspouts in Hungary.[15, 16] Propagation speed, path widths and lengths of seventeen tornadoes were examined by

Kecskés[17] between 1889 and 1972. These cases were found less violent then the American ones. His definition did not include the non-mesocyclonic tornadoes. Horvath[18] showed three tornado cases and presented how supercells and mesocyclone tornadoes can form. The non-mesocyclonic tornadoes were not mentioned in his paper.

The first documented non- mesocyclonic funnel cloud and short explanation of this phenomenon was published in Hungary in 2002. That tornado approached the ground for 300m and developed under a growing cumulus.[19] Sárközi[20] analyzed eighteen well-documented tornado cases especially from the viewpoint of damages and synoptic climatology. However, the terms of mesocyclone or supercell were not included in his study. The first detailed paper about non-supercell tornadoes in Hungary was published by Polyánszky and Molnár.[21]

General characterization

In 2005 two, in 2006 four, in 2008 seven and in 2009 eighteen vorticies were observed by volunteers. Some of these were classified as tornadoes (five F0, two F1, one F2) (Figs. 1 and 2) and the other 23 as funnel clouds. The growing number of observed cases can be related to the growing number of volunteers and the popularity of this activity. The observed vortices in 2008 and 2009 were mainly non-mesocyclonic ones, and only a smaller part of all observed phenomena were associated with mesocyclones of supercells or intense outflows (e.g., gustnadoes).[22] In all examined cases, the vortices developed along wind shift or frontal boundaries and the 0-6 km and 0-1 km wind shear was about 10 m/sec or less in their environment. Cases associated with fast moving meso- or synoptic-systems (e.g., fast moving cold fronts or linear storm systems) were not examined.

The strongest tornado, rated F2, occurred in Tyukod on 17 July 2005. It threw a container (weighs 9 tons) about 5-6 meters. It had a path length of 200m with a path width of 30m. The synoptic setting of its evolution differed from the others, because it formed along a slow-moving weak cold front that propagated at a speed of about 20-30 km/h. One of the two F1 tornadoes developed in Ipolytarnóc on 24 August 2008 and devastated with a maximum path width of 80-120 m and a path length of 200-300 m. It caused damages to roof-timbers and firewalls of twenty-two houses. The other one was formed in Nagybánhegyes on 11 May 2006 and caused 1-2 million HUF damage in a cemetery and in several houses. It tore out two healthy pines, which were 60-70 cm in diameter and were 10 m high. One of the six F0 tornadoes occured in Onga and it lifted up a plastic projecting roof and a piece of a slate roof to 200-250 m high and it threw them 300 m away from their original place. However, only a fraction of these caused effective damages, many of them were rated only by photos, because they occurred far from built-up areas. Therefore, some of the funnel clouds may have reached the F0 intensity.

The parent clouds of these vortices were usually cumuli or cumulus congestuses that often evolved into thunderstorms at a later stage. These parent clouds were mostly in the developing stage with inferred strong updrafts often owing to the flat, dark cloud base. In most cases, a precipitation echo appeared in the radar images around at the time of the observation. The radar reflectivity values were in the range between 25 dBZ and 58 dBZ nearby the observations, and the convective cells appeared as individual ones or embedded in the stratiform rain on the radar images. The radar echoes indicated the place of the event, hence the region of the ascending currents. Often at the same time, many funnel clouds were observed to develop usually for a short while only, but some of them existed for half an hour and did not change place. The intensive precipitation started usually around the observation of the intense vortices. The vortices associated with a non-mesocyclonic environment occurred between 0800 UTC and 1730 UTC, their maximum of occurrence was between 1200 UTC and 1500 UTC.

Synoptic setting and parameters

All cases occured in environments characterized by cyclonic curvature of isobars or, to a lesser extent in flat pressure areas (no pressure gradient). The vortices developed along mesoscale boundaries that could be identified usually on the surface map; on the mesoscale and often on synoptic scale, too. Sometimes these boundaries could be stationary, occluded or cold fronts. From the total number of 31 cases, the synoptic setting, involved in 18 events, consisted of a closed upper low (Fig. 3). The center of the closed upper low was normally located 200-400 km far from the events. The other events had the following synoptic features: in 2 events, a closed upper low; in 8 events, a long-wave trough (Fig. 4) and in 3 events, a short-wave trough (Fig. 5).

One third of the cases occured between 26/06/2009 and 28/06/2009, when 3-4 funnel clouds a day were observed in Hungary. During that period, there was a flat pressure area on the ground and a closed upper low near the Carpathian basin (Fig. 3). By the 29th, as the upper low flattening and moved 300-400 km to southeast, the number of events was halved. In the cases of the closed upper low and sufficiently moist environment, a mesoscale vortex was visualized on the radar images owing to the precipitation echoes over the Carpathian Basin. The events often appeared along the virtual axis of this vortex.

To investigate these cases, several analysis fields (MSL, moisture convergence, convergence at 10 m and between 0-1 km, 0-2 km vertical temperature gradient, 0-3 km section of surface based CAPE, vorticity at 10 m, 0-6 km average vorticity, LCL, 0-3 km storm relative helicity) and vertical profiles were used.

The aim of the study was to examine and to compare the analysis of undisturbed environmental conditions of these phenomena and, in this way, to understand the substantial processes; the aim was not to model the vortices in high resolution. Therefore, the analyses were made from a hydrostatic run of WRF ARW 3.1.1 model with 10 km horizontal resolution and from the surface information of the

automatic measurement network of the Hungarian Meteorological Service.

The model was set up as follows. The domain was centered at 47.2° N and 19.5° E with 10 km grid distance and the size of the grid was 85x65. The digital filter initialization allowed for the reduction in the model "spin-up" time during the early stages of integration due to a mass/momentum imbalance in the initial conditions. For the cumulus physics, the Kain-Fritsch scheme was applied.[23] The WSM Single-Moment 5-class microphysics scheme was used, that allowed for mixed-phase processes and super-cooled water.[24] For the planetary boundary layer, the Mellor-Yamada-Janjic scheme was used, that is the operational scheme of NAM model.[25] The applied land-surface physics scheme was the Noah Land Surface Model that includes the Unified NCEP/NCAR/AFWA scheme with soil temperature and moisture in four layers, fractional snow cover, and frozen soil physics and vegetation effects.[26]

Data were assimilated to the WRF fields. About 100 surface temperature and relative humidity, wind direction, wind speed at 10 meters and, approximately, 32 air pressure data. The initial and lateral conditions were obtained from the analysis and forecast of GFS with horizontal resolution of 0.5 and 1 degrees. In this study, the CAPE and 0-3 km CAPE were computed using the thermodynamic path of the surface based parcel.

Overviewing all the cases, the most important analysed parameters (the 0-3 km sbCAPE, convergence and moisture convergence at 10 m and 0-1 km and vorticity at 10 m) were found to overlap, but the others appeared less useful. The sbCAPE values were between 150 J/kg and 1800 J/kg, the 0-3 km CAPE was 50 - 300 J/kg and the 0-2 km lapse-rate was 6.5 – 10 ^{o}C. In the environment of the tornadoes, these values of CAPE, 0-3 km CAPE and the lapse-rate were at least 150 J/kg, 125 J/kg and 7-10 ^{o}C, respectively. These parameters were not good discriminators between the category of funnel clouds and tornados rated F0. However, in the cases of two F1 tornadoes, the values of the 0-3 km sbCAPE were especially high (250-300 J/kg); the other quantities were overlapped and, also, large. However, the parameters showed smaller values in the cases of F2 tornado (e.g., 150 J/kg sbCAPE), that formed in the environment of weak deep-layer and low-level shear (< 10 m/s). It can be assumed that the processes related to the moving cold front could play a role in the weakness. The LCL height ranged between 500 m and 1750 m, and it was especially low when the 0-2 km lapse-rate was below 7.5 ^{o}C. The presence of small convective inhibition (CIN) allowed the realization of CAPE.

The best documented and most interesting non-mesocyclone case in this study was reported from Ipolytarnóc. The previous night, a cold front passed trough the Carpathian Basin and behind it a strong stationary wind shift boundary developed on the lee side of the Carpathians on 24 August 2008 (Fig. 6). In the region of Ipolytarnóc, the diurnal heating was more intense and the dewpont did not decrease compared to other places during the day, so this area was protected from the macroscale impacts. The 0.5 degree base radar reflectivity image at 1037 UTC showed the development of a shower with 30-35 dBZ reflectivity (Fig. 7) along the boundary that moved to the southeast parallel to the boundary and the shower evolved to a multicell thunderstorm over Ipolytarnóc at the time of tornado observation at 1052 UTC (Fig. 8). Thus, the echo intensity increased around the observation of the intense vorticity and the echo could develop at the intersection of the thunderstorm outflow boundary and the wind shift boundary. The temperature, dewpoint and the 0-3 km sbCAPE was the highest and the other parameters were significant in Ipolytarnóc for several hours (Figs. 9 to 14). Thus, a vigorous developing updraft was juxtaposed with a pre-existing vertical vorticity circulation along the convergence.

The cell formed 100 km southwest of the Budapest radar. However, the Doppler velocity data was not useable for identifying the vorticity in the mid- or low-level. So, the classifying of this case occurred on the basis of photos, videos and survey of damages.

Conclusions

The calculated parameters were not good discriminators on the strength of the studied funnel clouds or F0 tornadoes, but many of them (e.g., 0-3 km sbCAPE, vorticity at 10 m) were found to overlap and had high values in the environment of two F1 tornadoes. On the basis of these parameters and the synoptic situation, one can evaluate the potential of the phenomena in question. On the basis of these thermo-dynamical parameters, the conditions of the environment seemed not so significant. The smaller scale processes were not examined in detail, however they were typical. The intensive precipitation started usually around the observation of the intense vortices. Thus, it may be assumed that the smaller scale thunderstorm outflow boundaries can enhance the pre-existing vertical circulations along wind shift boundaries. Therefore, the dynamic processes may play an imortant role in this type of tornado development or strengthening by thermo-dynamical processes. From knowledge of the studied environmetal conditions and synoptic settings, we conclude that these types of tornadoes are the majority of relatively weak tornadoes in Hungary.

Acknowledgements

The authors would like to thank Kálmán Csirmaz, Ákos Molnár, Gergely Leviczky, Péter Kardos.

References

[1]Fujita, T.T., 1981: Tornadoes and downbursts in the context of generalized planetary scales. *J. Atmos. Sci.*, **38**, pp. 1511-1534.

[2]Wakimoto, R. M., and J. W. Wilson, 1989: Non-supercell tornadoes. *Mon. Wea. Rev.*, **117**, pp. 1113-1140.

[3]Brady, R.H., and E.J. Szoke, 1989: A case study of non-mesocyclone tornado development in Northeast. Colorado: Similarities to waterspout formation. *Mon. Wea. Rev.*, **117**, pp. 843-856.

[4]Caruso, J. M., and J. M. Davies, 2005: Tornadoes in non-mesocyclone environments with pre-existing vertical vorticity along convergence boundaries. *NWA Electronic Journal of Operational Meteorology*, June 2005.

[5]Bluestein, H. B.,1985: The formation of a "landspout" in a „broken line" squall line in Oklahoma. *Preprints, 14th Conference on Severe Local Storms*, Indianapolis, Amer. Meteor. Soc., pp. 312-315.

[6]Marquis, J. N., and Y. P. Richardson, 2006: Kinematic observations of mesocyclones along boundaries during IHOP. *Mon. Wea. Rev.*, **117**, pp. 1749-1768.

[7]Lee, B. D., and R. Wilhelmson, 2000: The numerical simulation of non-supercell tornadogenesis. Part III: Tests investigating the role of CAPE, vortex sheet strength, and boundary layer vertical shear. *J. Atmos. Sci.*, **57**, pp. 2246–2261.

[8]Sinclair, P. C., 1969: General characteristics of dust devils. *J. Appl. Meteor.*, **8**, pp. 32-45.

[9]Rennó, N. O., M. L. Burkett, and M. P. Larkin, 1998: A simple thermodynamical theory for dust devils. *J. Atmos. Sci.*, **55**, pp 3244–3252.

[10]Keul, A. G., Sioutas, M., Szilagyi, W., 2009: Prognosis of Central-Eastern Mediterranean waterspouts. *Atmos. Res.*, **93**, pp. 426-436.

[11]Lemon, L.R., 1977: New severe thunderstorm radar identification techniques and warning criteria: A preliminary report. *NOAA Tech. Memo. NWS NSSFC-1* (NTIS Accession No. PB-273049), pp. 60.

[12]Rassmussen, E. and D. O. Blanchard, 1998: A baseline climatology of sounding-derived supercell and tornado forecast parameters. *Wea. Forecasting.*, **13**, pp. 1148-1164.

[13]Thompson, R. L., R. Edwards, J. A. Hart, K. L. Elmore, and P. Markowski, 2003: Close proximity soundings within supercell environments obtained from the Rapid Update Cycle. *Wea. Forecasting.*, **18**, pp. 1243-1261.

[14]Davies-Jones, R., D. Burgess and M. Foster, 1990: Test of helicity as a tornado forecast parameter. *Proc. 16th Conf. Severe Loc. Storms*, Kananaskis Park, Albert, Canada, Amer. Meteor. Soc., pp. 588-592.

[15]Fábián, T., 1973: A Nagyatádi tornádórol. *Légkör.*, **18**, pp. 38-43.

[16]Bartha, I., 1972: Tornádószerű víztölcsér a Balatonon. *Légkör.*, **17**, pp. 70-74.

[17]Kecskés, L., 1988: Tornádók és előfordulásuk Magyarországon. *Légkör.*, **33**, pp. 27–30.

[18]Horváth, Á., 1997: Tornádó! *Légkör.*, **42**, pp. 2-8.

[19]Kósa-Kiss, A., Horváth, Á., 2002: Tornádótölcsér Nagyszalonta határában. *Légkör.*, **47**, pp. 13.

[20]Sárközi, Sz., 2007: A systematic approach to synoptic tornado climatology of Hungary for the recent years (1996-2001) based on official damage reports. *Atmos. Res.*, **83**, pp. 263-271.

[21]Polyánszky, Z., and Á. Molnár, 2007: Nem mezociklonális tornádók Magyarországon. *Légkör.*, **52**, pp. 35-40.

[22]Doswell, C.A. III, and D.W. Burgess, 1993: Tornadoes and tornadic storms: A review of conceptual models. *The Tornado: Its structure, Dynamics, Prediction, and Hazards*. Geophys. Monogr., No. 79. Amer. Geophys. Union, pp. 161-172.

[23]Kain, John S., 2004: The Kain–Fritsch Convective Parameterization: An Update. *J. Appl. Meteor.*, **43**, pp. 170–181.

[24] Hong, Song-You, Jimy Dudhia, Shu-Hua Chen, 2004: A Revised Approach to Ice Microphysical Processes for the Bulk Parameterization of Clouds and Precipitation. *Mon. Wea. Rev.*, **132**, pp. 103–120.

[25]Janjic, Z. I., 1996: The Mellor-Yamada level 2.5 scheme in the NCEP Eta Model. *11th Conference on Numerical Weather Prediction*, Norfolk, VA, 19-23 August 1996; American Meteorological Society, Boston, MA, pp. 333-334

[26]Chen, F., and J. Dudhia, 2001: Coupling an Advanced Land Surface–Hydrology Model with the Penn State–NCAR MM5 Modeling System. Part II: Preliminary Model Validation. *Mon. Wea. Rev.*, **129**, pp. 587–604.

Figure 1 The distribution of vorticies in Hungary. In 2005 two, in 2006 four, in 2008 seven and in 2009 eighteen events were observed by volunteers. Some of these can be classified as tornadoes (five F0, two F1, one F2) and others as funnel clouds.

Figure 2 On 24 August 2008 in Ipolytarnóc, a non-mesocyclone tornado was rated F1 damaged with a maximum path width of 80-120 m and a path length of 200-300 m. It caused damages to roof-timbers of 22 houses and pulled down the partition-wall. (photo by Berkó Ernő, szupercella.hu).

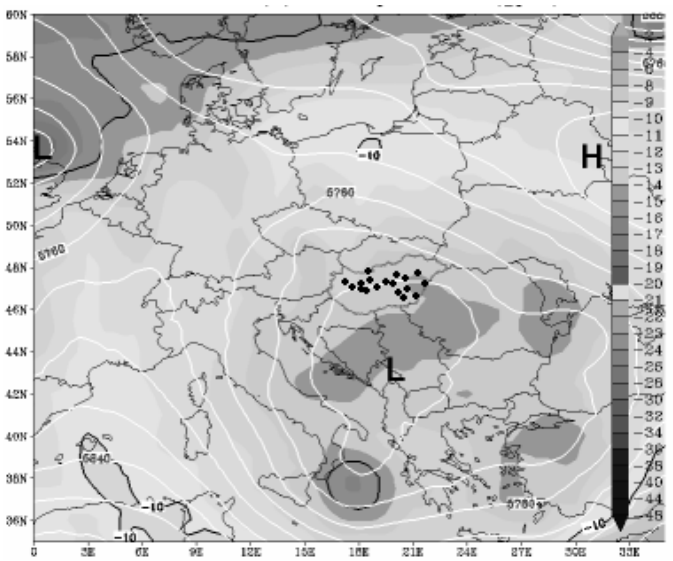

Figure 3 Temperature and geopotential fields at 500 hPa. Typical synoptic setting at 500 hPa (closed upper low) that occurred, from the total number of 31 events, during 18 events. The black points indicate the locations of the events.

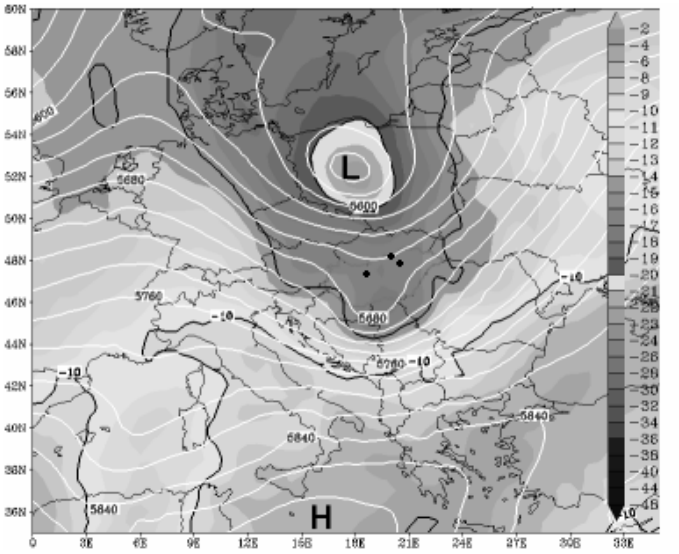

Figure 5. Temperature and geopotential fields at 500 hPa. Typical synoptic setting at 500 hPa (short-wave trough) that occurred, from the total number of 31 events, during 3 events. The black points indicate the location of the events.

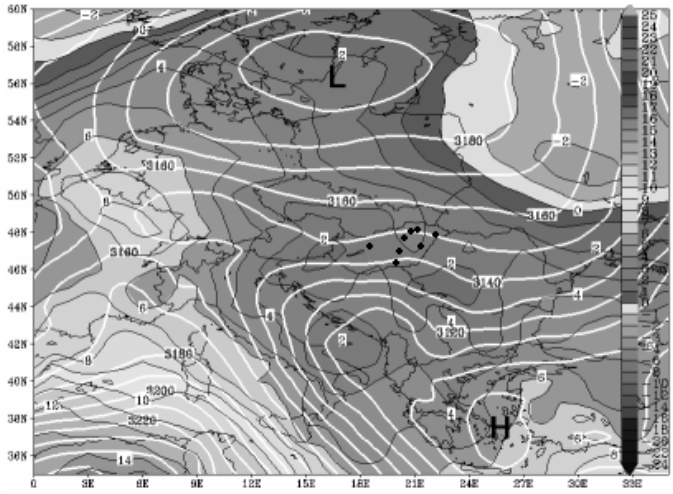

Figure 4 Temperature and geopotential fields at 500 hPa. Typical synoptic setting at 500 hPa (long-wave trough) that occurred, from the total number of 31 events, during 8 events. The black points indicate the location of the events.

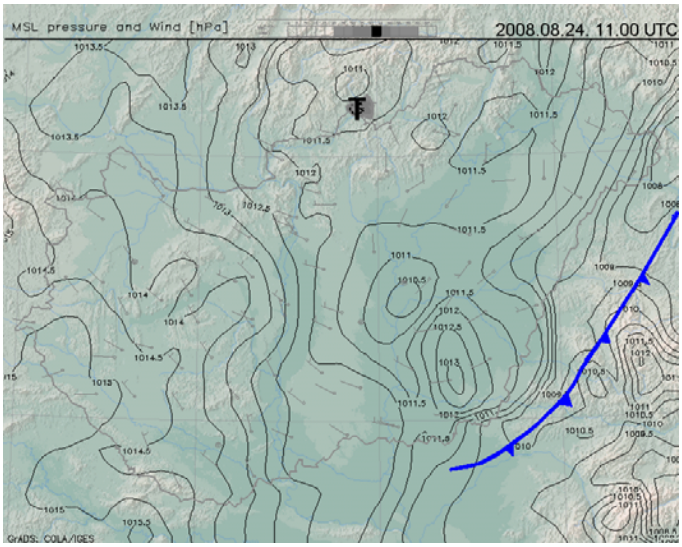

Figure 6. Synoptic setting at the ground. The previous night, a cold front passed trough thehe Carpathiana Basin and behind it a strong stationary wind shift boundary developed on the lee side of the Carpathians. The tornado (T) developed over Ipolytarnoc at 1052 UTC on 24 August 2008.

Figure 7 The 0.5 degree base radar reflectivity image at 1037 UTC showing development of a shower with 30-35 dBZ reflectivity along the boundary.

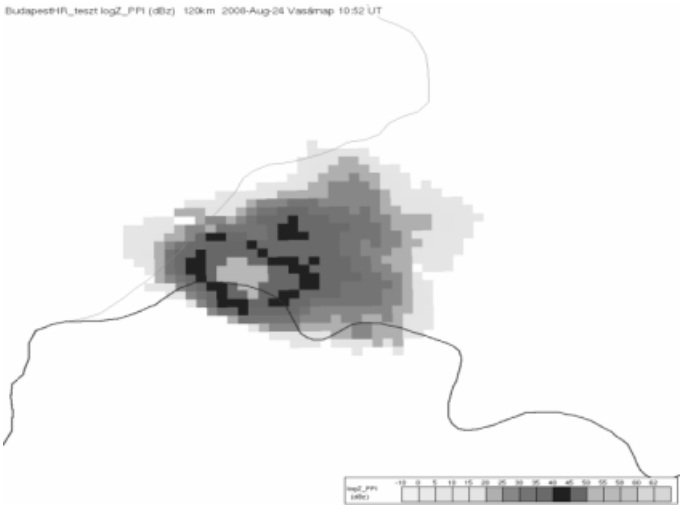

Figure 8 A thunderstorm formed over Ipolytarnóc and an F1 tornado was observed at 1052 UTC.

Editor's note: In Figures 9 through 14, the grey-shade fields that appear in the print copy appear in full-color in the online version found at journals.sfu.ca/ts/.

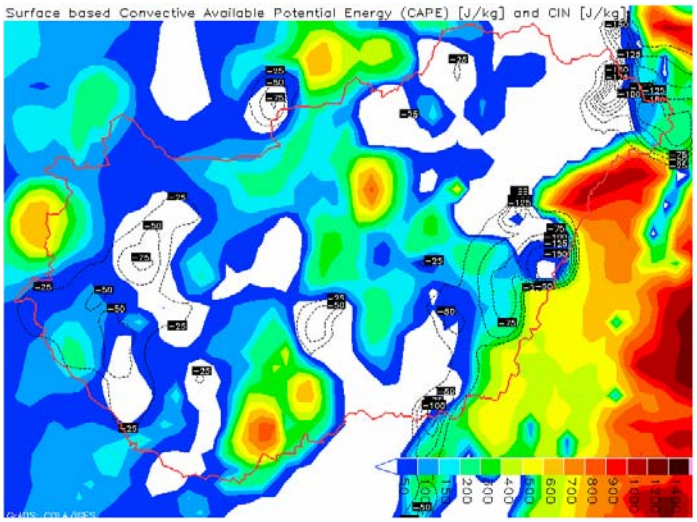

Figure 9 Surface-based CAPE and CIN analysis fields at 1000 UTC on 24 August 2008.

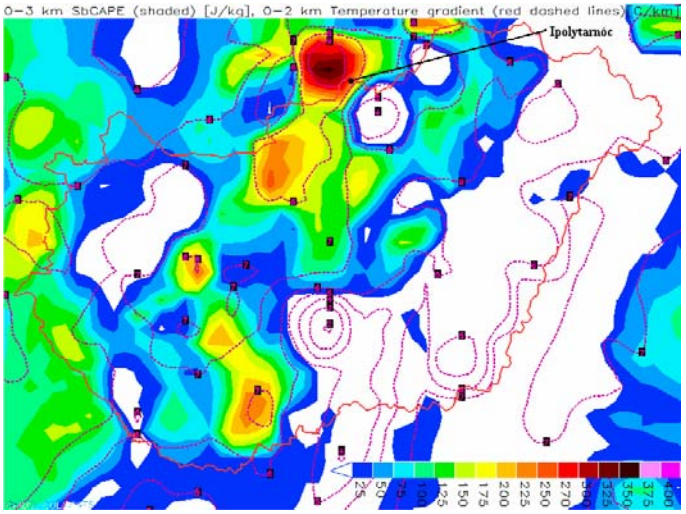

Figure 10 0-3 km surface-based CAPE and 0-2 km temperature gradient analysis fields at 1000 UTC on 24 August 2008.

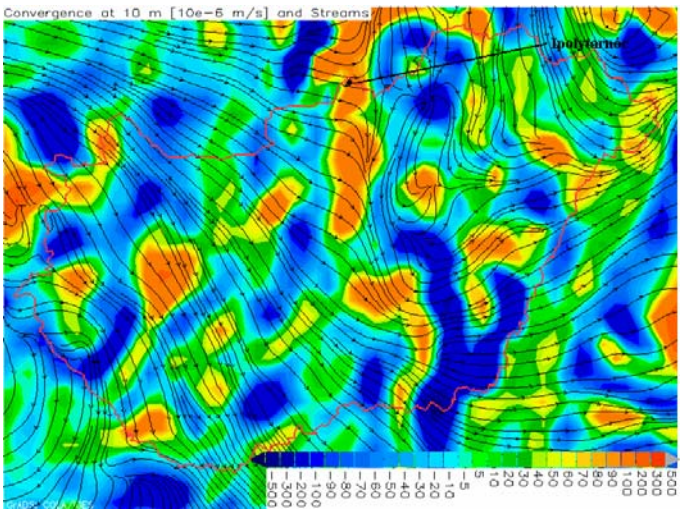

Figure 11 Convergence at 10 m analysis field at 1000 UTC on 24 August 2008.

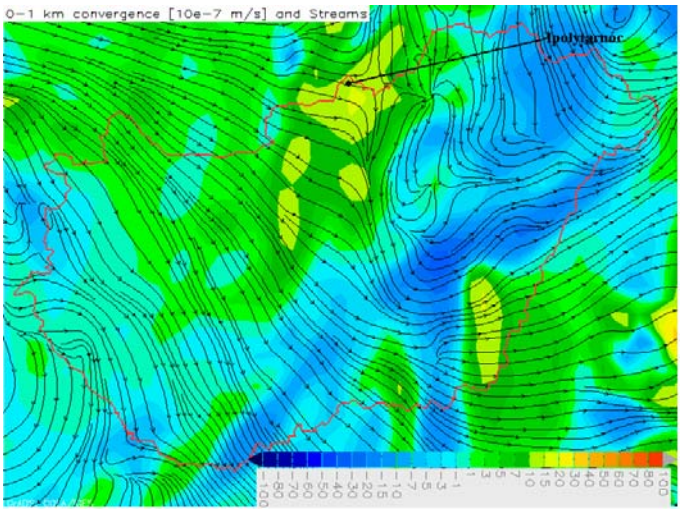

Figure 12 0-1 km convergence analysis field at 1000 UTC on 24 August 2008.

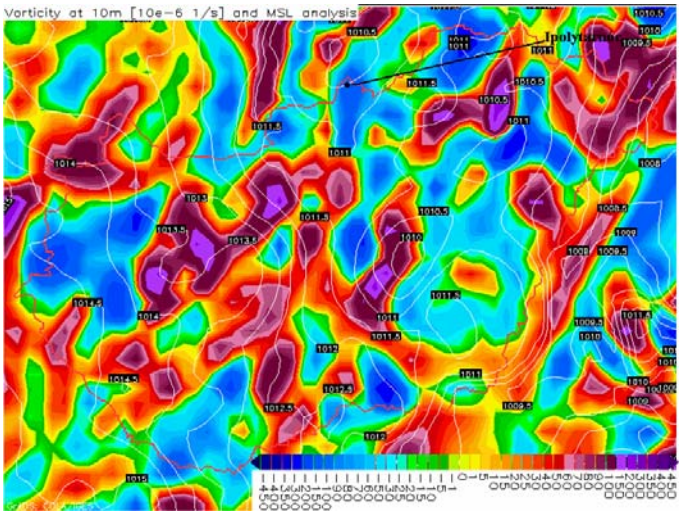

Figure 13 Vorticity at 10 m analysis field at 1000 UTC on 24 August 2008.

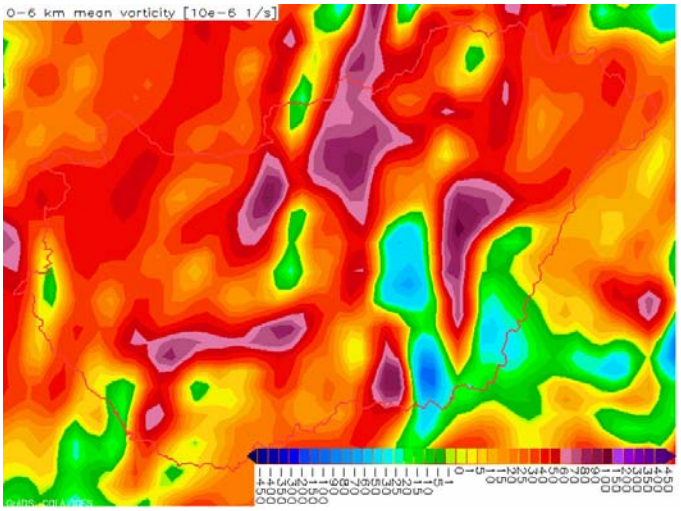

Figure 14 0-6 km mean vorticity analysis field at 1000 UTC on 24 August 2008.